PRELIMINARY MELT MODELS OF TROCTOLITE AND ANORTHOSITE CLASTS WITHIN NORTHWEST AFRICA 11303. A. L. Fagan[1] and J. Gross[2,3,4,5], [1]Geosciences and Natural Resources Dept., Western Carolina University, Cullowhee, NC 28723 (alfagan@wcu.edu), [2]Rutgers, State University of New Jersey, Department of Earth and Planetary Sciences, Piscataway, NJ 08854; [3]Dept. of Earth & Planetary Sciences, American Museum of Natural History, New York, NY 10024; [4]NASA, Johnson Space Center, Mail Code X12, Houston, TX, 77058; [5]Lunar and Planetary Institute, Houston TX 77058.

Introduction: The lunar highland crust is predominantly composed of igneous rocks that include the Ferroan Anorthosites (FANs, [e.g., 1]), the Mg-suite, and a proposed Magnesian Anorthosite (MAN, [e.g., 2-4]) suite that bridges the compositional gap between the former two suites. The troctolitic suite (troctolites, anorthositic troctolites, and troctolitic anorthosite) is a subset of the Mg-suite that are predominantly composed of plagioclase and olivine with little to no pyroxene. The troctolitic suites represented in the Apollo and meteoritic collections are distinct from one another, with the Apollo collection having a KREEP signature (i.e., rich in K, REE, and P [e.g., 5,6]) and the meteoritic samples lacking one [e.g., 3, 7-8]. Meteorites represent random samples of the lunar surface, therefore these samples suggest that the Mg-suite, of which the troctolitic suite is a subset, varies in the KREEP component across the lunar surface. To better understand the origin of these distinct members of the Mg-suite and their role in the evolution of the Moon, it is essential to conduct detailed chemical analyses of troctolitic suite samples from the Apollo and meteoritic collections.

In order to ascertain any genetic relationships between members of the troctolitic suite and related rock types (e.g., anorthosite), it is critical to examine the composition of the magmas, which are modelled as equilibrium liquids (EL). These EL can be determined using in-situ trace element compositions from plagioclase and partition coefficients derived for each unique analysis based on its An content (Ca/[Ca+K+Na]*100) using $C_L = \frac{C_S}{D}$, where C_L (i.e., EL) and C_S are the concentrations of a given element in the liquid phase and solid phase, respectively, and D is the partition coefficient. Plagioclase is an ideal phase to examine here, as it is on the liquidus for an extended time for these suites and therefore serves as a good measure for the changing liquid compositions, which can then be compared to compositions of other lunar lithologies to determine any similarities in parentage.

In this study, we focus on four clasts within lunar feldspathic regolith breccia Northwest Africa (NWA) 11303, a member of the sensu stricto NWA 8046 pairing group [9,13], which is composed of a range of angular isolated mineral grains and lithic clasts set in a dark, glassy groundmass [9] and contains several Si-bearing metals with exogenic provenances [10]. Many of the clasts within NWA 11303 have granulitic textures, and lithic clast types include anorthosites, impact melts, and mafic/gabbroic material [11].

Sample Description: Clast 1 (Fig. 1a) is an anorthosite, composed predominantly of plagioclase laths with intergranular olivine. Clast 2 (Fig. 1b) is a troctolite with a granular texture dominated by plagioclase, olivine, and lesser amounts of pyroxene. Clasts 6 (Fig. 1c) and 11 (Fig. 1d) are troctolites dominated by plagioclase with intergranular olivine, minor pyroxene, and varying amounts of ilmenite.

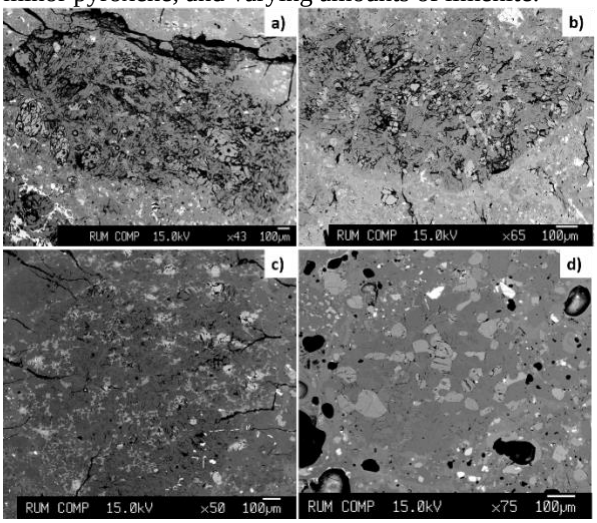

Fig. 1. *Backscattered electron images of clasts in this study: (a) Clast 1, (b) Clast 2, (c) Clast 6, (d) Clast 11.*

Methods: *Major and Minor Elements:* Backscattered electron (BSE) images and major and minor elements of plagioclase were quantified using the JEOL-8200 superprobe at Rutgers University's Department of Earth and Planetary Sciences (RU-EPS) using the following beam conditions: 15kV accelerating voltage, 25nA beam current, and defocused 5 µm beam. Peak times ranged from 10 to 40s per element. Standards included well characterized natural and synthetic materials.

Trace Elements: Trace elements were obtained using a Thermo Scientific iCAP Qc ICP-MS system equipped with a Photon Machines 193 nm laser ablation system at RU-EPS. Samples were ablated with a fluence of 5.3 J/cm^2, shot frequency of 10 Hz, dwell time of 10 ms for each element, and spot sizes of 50 to 60 µm. NIST glasses 610, 612, and 614 as well as BCR and BIR glasses were used as the internal and external standard, respectively, and were regularly analyzed throughout the run for continuous calibration and drift account.

Equilibrium Liquid Modelling: We employ a modified Bindeman method of determining partition coefficients by anorthite (An) content, which is based on the work of [13-14] and described in [15]. Here we use the updated experimentally-determined partition coefficients reported in [16-17] along with previously published data [13, 18-20]. The recent results of [16-17] are important to the EL modelling, as these represent some of the few experiments conducted at lunar-relevant oxygen fugacities and An content.

Results: Plagioclase from each clast are broadly similar (e.g., An_{avg} 96 to 97), but those in anorthosite (Clast 1) generally have lower FeO content (up to 0.13 wt %) than in troctolites (up to 0.33 wt%). For trace elements, Clast 11 generally has the highest Ba and Y (Fig. 2a). In contrast, Clasts 1 and 2 have similar Ba and Y, but are distinct in other trace elements, such as La and Ni (Fig. 2b). Chondrite-normalized Rare Earth Element (REE) patterns for all clasts are subparallel with the Clast 1 anorthosite analyses (blue lines) lying in the middle of the troctolite range (Fig. 2).

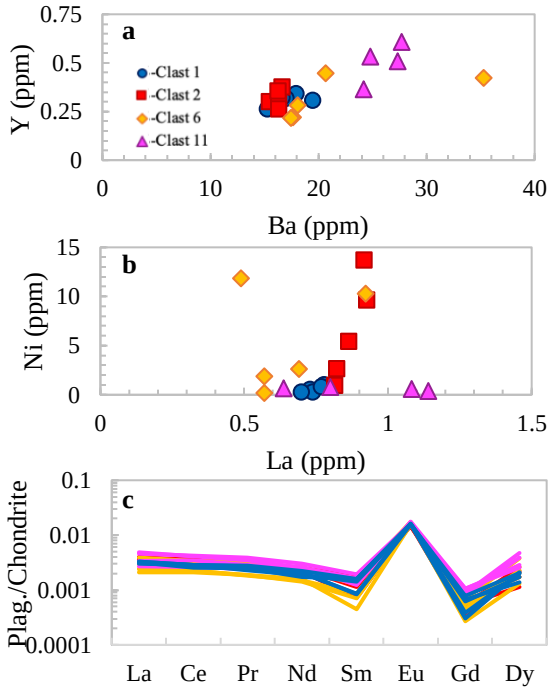

Fig. 2. *Trace element compositions of plagioclase in anorthosite (clast 1) vs troctolites (clasts 2,6,11).*

Modelling is ongoing, but preliminary results give broadly similar EL among the different clasts (Fig. 3). Consistent with Fig. 1, the chondrite-normalized EL for the anorthosite (clast 1) lies in the middle of the troctolite range (e.g., La_N, Fig. 3a). EL for selected published values of plagioclase from Apollo collection troctolites [21], anorthosites [21,22], and Mg-suite norites [6], as well as from a meteoritic anorthositic troctolite, NWA 10401 [23], were also calculated using the same method for comparison (Fig. 3b). The NWA 11303 EL are similar to NWA 10401, but less enriched in La than most of the represented Apollo samples; the chondrite-normalized Sm/Eu (Sm_N/Eu_N) ratio for the NWA 11303 clasts is similar to some of the Apollo samples, but falls on the lower range (Fig. 3).

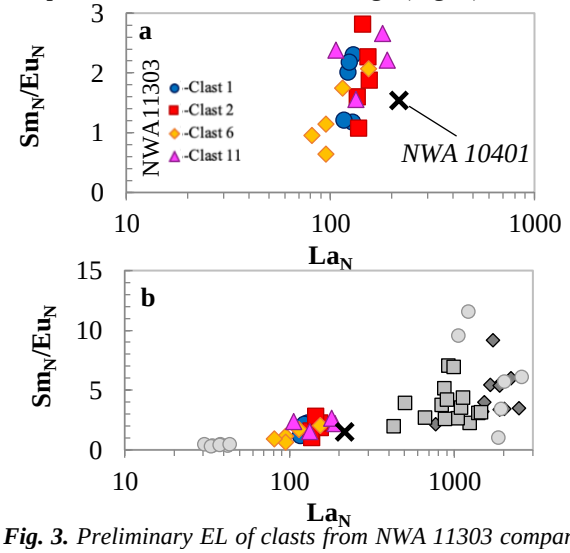

Fig. 3. *Preliminary EL of clasts from NWA 11303 compared with models of published plagioclase data for troctolites (grey diamonds [22]), anorthosites (grey circles [22,23]) and Mg-suite norites (grey squares [6]).*

Discussion and Implications: Data collection and modeling are ongoing, but results suggest that the plagioclase from the NWA 11303 are distinct from those of the Apollo collection, but broadly consistent with at least one other sample from the meteoritic troctolitic suite, which is consistent with the overall difference in bulk chemistry between the Apollo and meteoritic collections. Continued modelling may further elucidate why these suites are so distinct.

Acknowledgements: This work is supported, in part, by NASA grant 80NSSC19K0558.

References: [1]Warren P.H. (1990) *Am. Min. 75*, 46-58. [2]Lindstrom M.M. et al. (1984) *JGR., 89*, C41-C49. [3]Takeda et al. (2006). [4]Gross J. et al. (2014) *Am. Min., 99*, 1849-1859. [5]Papike J.J. et al. (1994) *LPSC 25*, 1045-1046. [6]Papike J.J. et al. (1996) *GCA 60*, 3967-3978. [7]Treiman et al. (2010) *MaPS, 45*, 163-180. [8]Pieters C.M. et al. (2011) *JGR. 116*, E00G08. [9]Meteoritical Bulletin Database. [10]Lunning N.G. & Gross J. (2019), *Met. Soc. 82*, Abs# 6076. [11]Lunning N.G. & Gross J. (2019), *LPSC 50*, Abs# 2407. [12]Korotev R., meteorites.wustl.edu/lunar/stones/nwa 8046.htm. [13]Bindeman I.N. et al. (1998) *GCA 62*, 1175-1193. [14]Blundy J.D. & Wood B.J. (1991) *GCA 55*, 193-209. [15]Fagan A.L. et al. (2017) *LPSC 48*, Abs# 2691. [16]Rapp J.F. et al. (2015) *LPSC 46*, Abs# 2878. [17]Dygert N. et al. (under rev.) *GCA*. [18]Blundy J. (1997) *Chem. Geol. 141*, 73-92. [19]Bindeman I.N. & Davis A.M. (2000) *GCA 64*, 2863-2878. [20]Aigner-Torres M. et al. (2007) *Contrib. Min. Pet. 153*, 647-667. [21]Shervais J.W. & McGee J.J. (1998) *GCA, 62*, 3009-3023. [22]Papike J.J. et al. (1997) *GCA 61*, 2343-2350. [23]Gross J. et al. (under rev.) *JGR*.